Discrete and extended metal-metal bonding

C. Hoch, C. Zheng, Hj. Mattausch, J. Nuss, L. Kienle, J. Köhler and A. Simon

The mercury-richest amalgam: Cs_2Hg_{27}

The synthesis of the mercury richest of all structurally known amalgams [1] and the elucidation of its crystal structure was enabled by an electrolysis technique developed for the growth of ammonium amalgam crystals [2]. Cs_2Hg_{27} crystallizes in an own structure type [3]. The cubic unit cell (space group *Im*-3, No. 204, $a = 16.557(4)$ Å) contains six formula units. The interatomic distances ($d_{Hg-Hg} = 298$ pm to 427 pm, $d_{Cs-Hg} = 368$ pm to 409 pm) and the coordination numbers ($CN_{Cs} = 20$) are very similar to those in known mercury-rich alkali metal amalgams.

The structure can best be described by a system of concentric polyhedra, as shown in Fig. 46 for the asymmetric unit. The central Hg(7) atom is surrounded by 12 Hg(3) atoms, forming an icosahedron. It is enclosed by 20 Hg atoms (12 Hg(5) + 8 Hg(6)) which form a pentagondodecahedron, surrounded by a cuboctahedron built from 12 Hg(4) atoms. The outermost Hg polyhedron is a strongly distorted truncated icosahedron of 60 atoms (12 Hg(1) + 48 Hg(2)). This cluster of 105 mercury atoms is enclosed by a slightly distorted sodalith cage of 24 cesium atoms. The entire crystal can be assembled from those sodalith cages via sharing of all faces. Each Cs atom belongs to four sodalith cages, and the Hg_{105} clusters are condensed via the puckered six-membered outermost rings beneath the hexagons of the sodalith cages. The sum formula of the structure therefore is $Cs_{24/4}Hg(7)_1Hg(3)_{12}Hg(5)_{12}Hg(6)_8Hg(4)_{12}Hg(1)_{12}Hg(2)_{48/2} = Cs_6Hg_{81}$. The structure of Cs_2Hg_{27} is closely related to the atomic arrangement in Bergman phases, well-known 1/1 approximants of quasi-crystalline ternary intermetallic structures. Deviations of the atomic coordinates of the atoms Hg(1), Hg(2) and Hg(4) with respect to the Bergman structure leads to a different polyhedral system and hence to a regular crystalline structure.

The formal reduction of all Hg atoms inside the Cs sodalith cage to one big sphere reveals the topological similarity of the structures of Cs_2Hg_{27} and α-AgI. In the α-AgI structure the I atoms have bcc type packing, and the partially occupied Ag-sites form undistorted sodalith cages.

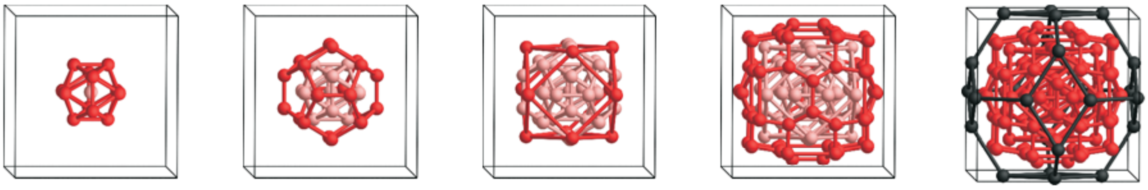

Figure 46: 'Aufbau principle' of the structure of Cs_2Hg_{27} (see text).

$La_6Br_{10}Fe$: Cluster with M_6X_{12}/M_6X_8 type environment

M_6X_8 and M_6X_{12} units are textbook examples of transition metal clusters. In the M_6X_{12} cluster, all edges of the M_6 octahedron are bridged by non-metal atoms X. In the M_6X_8 cluster, all faces are capped by X atoms. These clusters can be linked or condensed to chains, sheets or three dimensional frameworks. In the case of M = rare earth metal the M_6X_{12} type arrangement is generally chosen, and the cluster is stabilized by endohedral atoms, e.g., C up to Au.

The structure of $La_6Br_{10}Fe$ is a first example of a mixed M_6X_8/M_6X_{12} type cluster [4]. It contains the familiar octahedral La_6Fe unit, however, only nine Br atoms lie above edges and three above faces of the octahedron as shown in Fig. 47(a). Out of the 12 Br atoms above the octahedron apices, 4 also bridge the edge or cap the face of an adjacent La_6Fe octahedron, and 8 are shared with two other La_6 octahedra, linking one corner and bridging one edge or capping one face of these two octahedra as shown in Fig. 47(b).

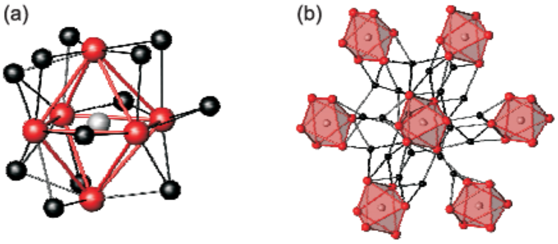

Figure 47: (a) La_6Fe octahedron coordinated by Br atoms in the $La_6Br_{10}Fe$ structure, (b) Interconnection of the La_6Fe units.

Neglecting the Br atoms above the apex atoms the discrete cluster has the composition $La_6Br^{e}_{9}Br^{f}_{3}Fe$ where e and f denote positions above the edges and faces of the octahedron, respectively. As the e-type atoms Br1 and Br10 are shared between adjacent clusters in the same functionality, the formula $La_6Br^{e}_{5}Br^{e}_{4/2}Br^{f}_{3}Fe = La_6Br_{10}Fe$ results.

The pronounced asymmetry of the Br coordination polyhedron around the La_6Fe octahedron has two important consequences. First, the La octahedron is heavily distorted, in first approximation squeezed along a four-fold axis. Second, the rock salt type arrangement, i.e., the common close-packing of Br atoms and La_6Fe units as normal with the M_6X_{12} type cluster is disrupted. The distortion could be of electronic origin. A formal electron partition of $(La^{3+})_6(Br^-)_{10}Fe^{2-} \cdot 6e^-$ shows that there are 16 cluster electrons in the La_6Fe octahedron including those of Fe^{2-}, and 6 electrons form metal-metal bonds in the La_6 cage. As four electrons would occupy the degenerate t_{1u} orbitals in a regular cluster the Jahn-Teller effect clearly favors a distortion of the cluster as observed in $La_6Br_{10}Fe$.

Undulated and planar sheets of $La_6(C_2)$ units

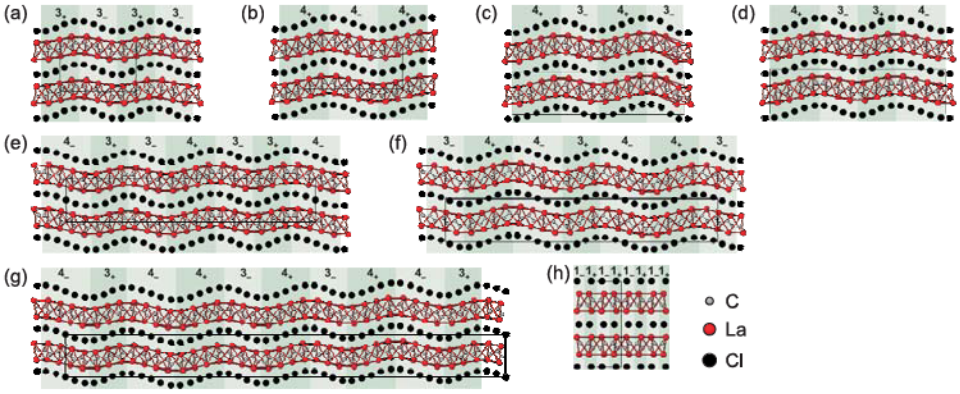

Figure 48: Projections of the crystal structures of (a) $La_6(C_2)_3Cl_4$, (b) $La_8(C_2)_4Cl_5$, (c),(d) $La_{14}(C_2)_7Cl_9$, (e) $La_{20}(C_2)_{10}Cl_{17}$, (f) $La_{22}(C_2)_{11}Cl_{14}$, (g) $La_{36}(C_2)_{18}Cl_{23}$ and (h) $La_2(C_2)Cl$ (h) along [001]. The number of ribbons (3,4) and their orientation (+, -) are highlighted by bright and dark green.

In the system of lanthanum ethanide chlorides we found a series of new compounds with the chemical formulae $La_6(C_2)_3Cl_4$, $La_8(C_2)_4Cl_5$, $La_{14}(C_2)_7Cl_9$, $La_{20}(C_2)_{10}Cl_{17}$, $La_{22}(C_2)_{11}Cl_{14}$, $La_{36}(C_2)_{18}Cl_{23}$ and $La_2(C_2)Cl$ [5]. The crystal structures are composed of distorted C_2 ('ethanide') centered La_6 octahedra which are condensed into chains via common edges. Three (3) and/or (4) such chains join into ribbons. Finally, the 3-, 4-ribbons are condensed into undulated (up: (+), down: (−)) sheets with the Cl atoms between them, as denoted in Fig. 48.

The compounds are members of the series $(La_6(C_2)_3Cl_4)_m\ (La_8(C_2)_4Cl_5)_n$ with $m = 1$, $n = 0$ (Fig. 48(a)), $m = 0$, $n = 1$ (Fig. 48(b)), $m = 2$, $n = 2$ (Fig. 48(c), 46(d)), $m = 4$, $n = 2$ (Fig. 48(e)), $m = 2$, $n = 4$ (Fig. 48(f)), $m = 4$, $n = 6$ (Fig. 48(g)). HRTEM investigations confirm the X-ray results. For $La_{14}(C_2)_7Cl_9$ a second modification is found (Fig. 46(c)). Arrangements of greater complexity so far have not been observed. The examination of the number of combinations with two different ribbon sizes in alternating orientations, +, −, using a combinatorial approach including redundancy based on symmetry resulted in 110 possible structural variants for a sequence of up to 10 ribbons. In the meantime we found compounds of a new series based on 4- and 5-ribbons, namely $Ce_{18}(C_2)_9Cl_{11}$ with the sequence $\cdots 4_-\ 5_+\ 4_-\ 5_+ \ldots$ and $Ce_{26}(C_2)_{13}Cl_{16}\cdots$ with $\cdots 5_-\ 4_+\ 4_-\ 5_+\ 4_-\ 4_+\ 5_- \cdots$. Obviously, we face the tip of an iceberg with these phases.

---

[1] *Deiseroth, H.J.* Progress in Solid State Chemistry **25**, 73–123 (1997).

[2] *Hoch, C and A. Simon.* Zeitschrift für anorganische und allgemeine Chemie **632**, 2288–2294 (2006).

[3] *Hoch, C and A. Simon.* Zeitschrift für anorganische und allgemeine Chemie **634**, 853–856 (2008).

[4] *Zheng, C., Hj. Mattausch, C. Hoch and A. Simon.* Inorganic Chemistry **47**, 2356–2361 (2008).

[5] *Mattausch, Hj., A. Simon, L. Kienle, J. Köhler, C. Hoch and J. Nuss.* Zeitschrift für anorganische und allgemeine Chemie **634**, 2765–2776 (2008).